



Cornell University

The semidiurnal variation in GPS-derived zenith neutral delay

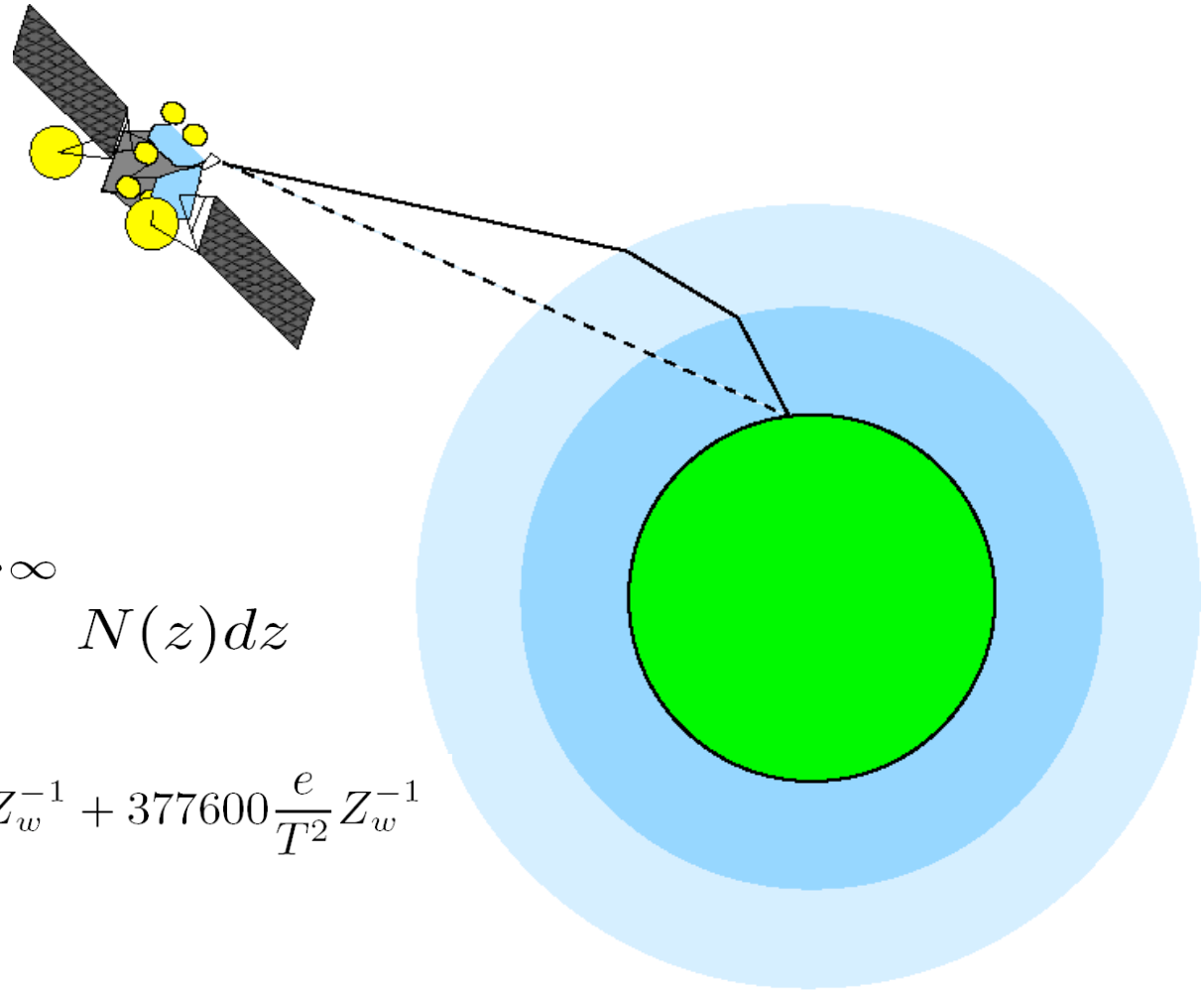
Todd E. Humphreys, Michael Kelley, Norbert
Huber, and Paul M. Kintner, Jr.

Cornell University

GRL Vol. 32, December 2005

IGS Workshop 2006, Darmstadt

Zenith Neutral Delay from the International GNSS Service

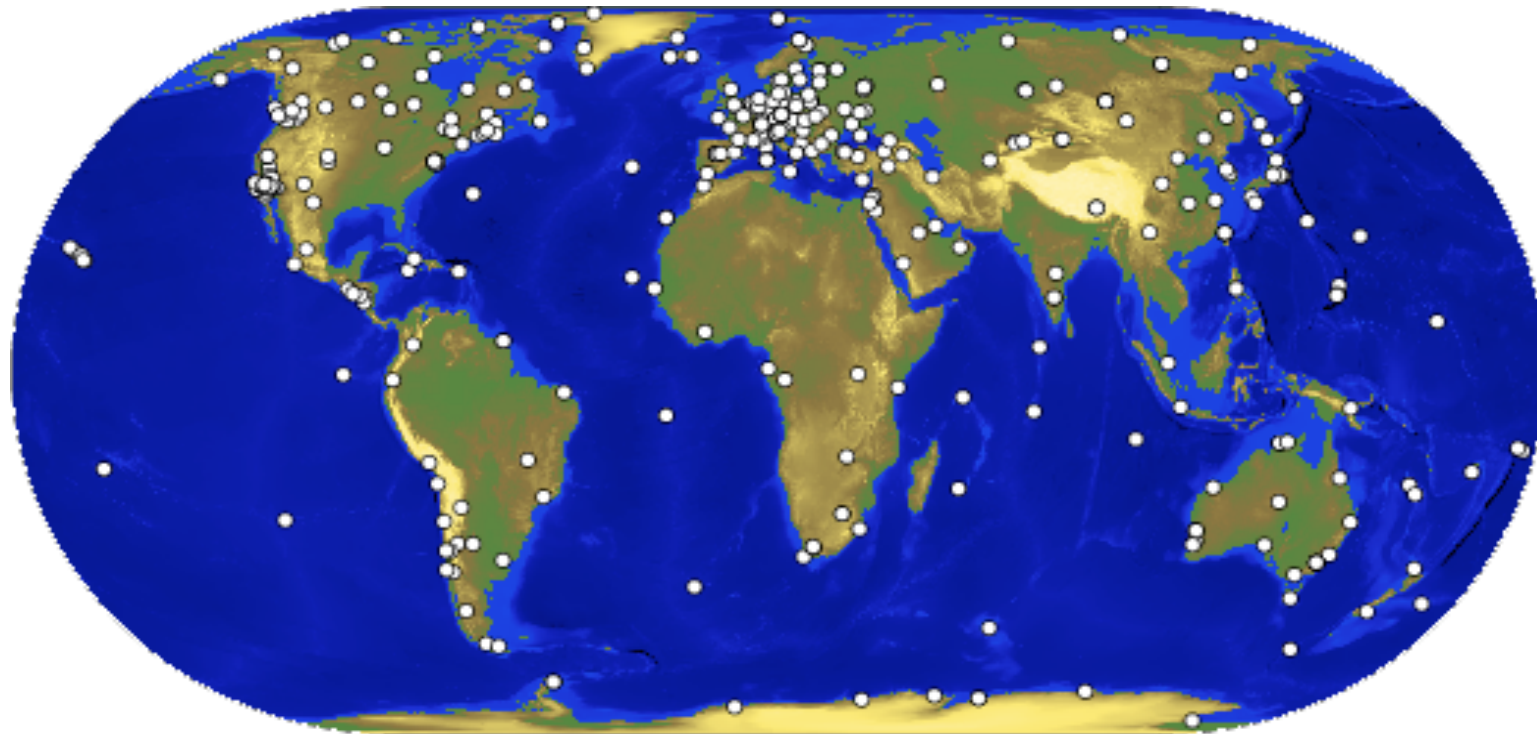


$$\tau^z = ct^z = 10^{-6} \int_0^{\infty} N(z) dz$$

$$N = 222.76\rho + (17 \pm 10) \frac{e}{T} Z_w^{-1} + 377600 \frac{e}{T^2} Z_w^{-1}$$

$$\tau^z = \tau_h^z + \tau_w^z$$

Zenith Neutral Delay from the International GNSS Service



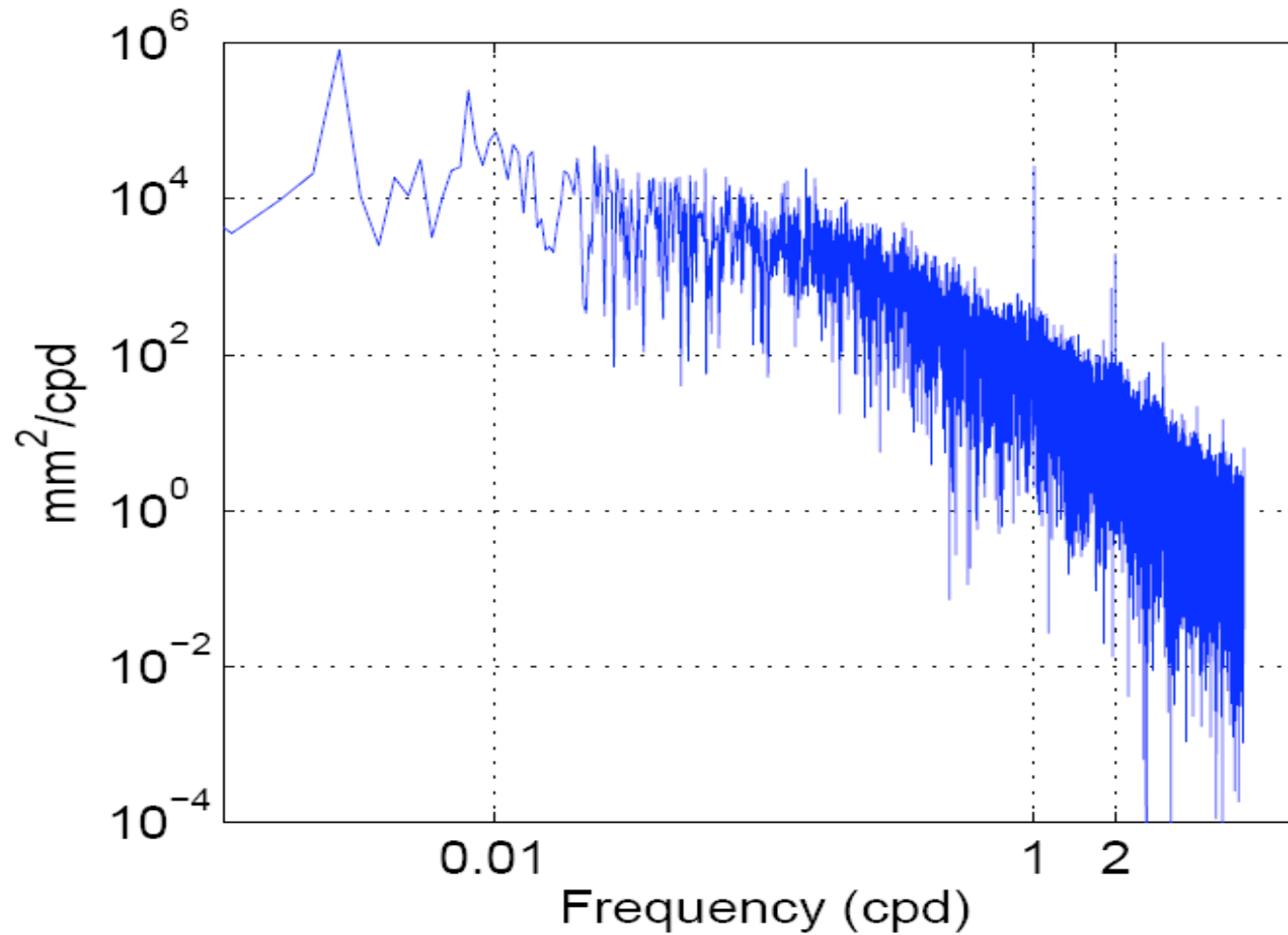
IGS 2008 May 5 17:34:17

Zenith Neutral Delay from the International GNSS Service

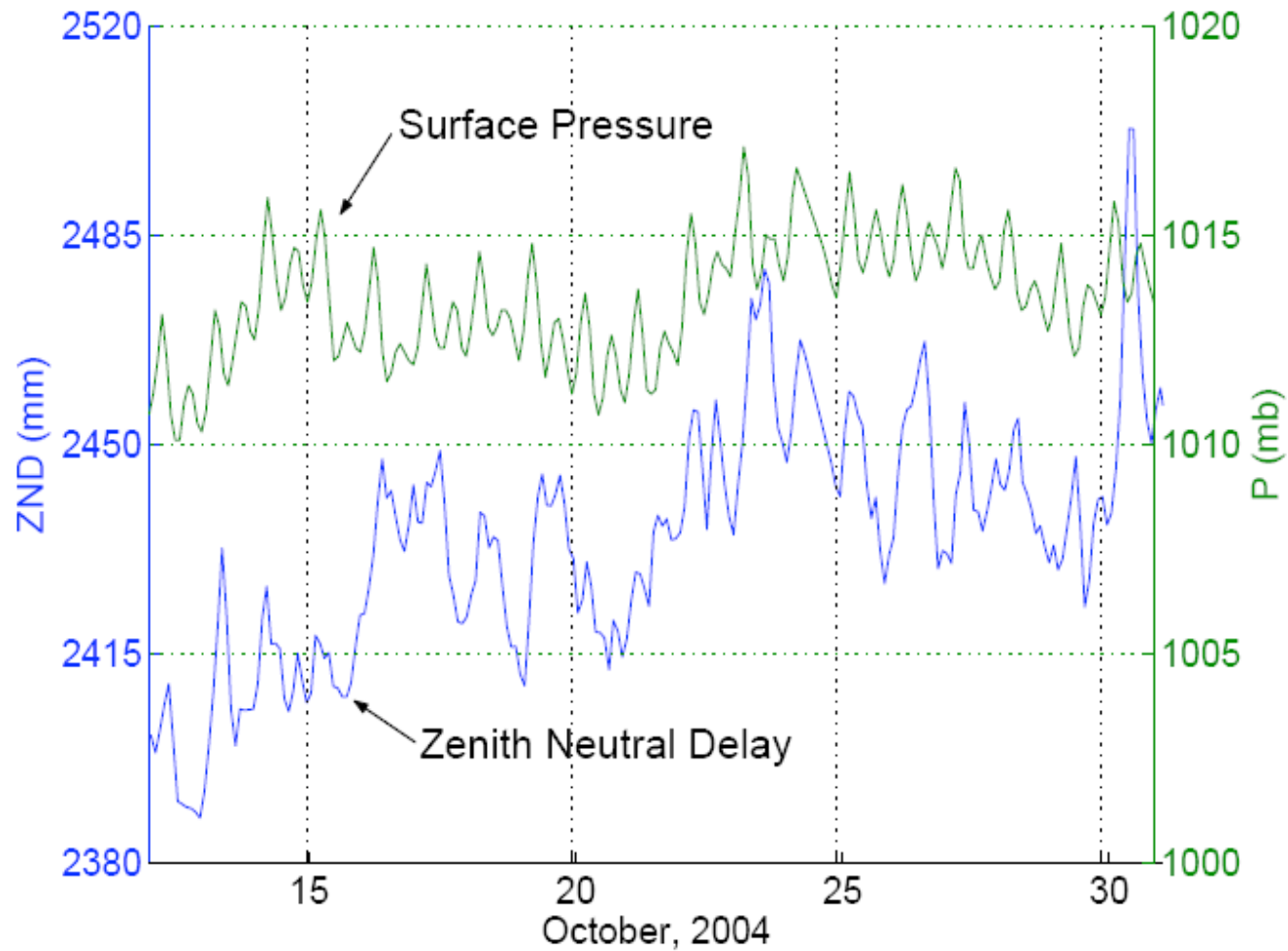


IGS 2008 May 5 17:34:17

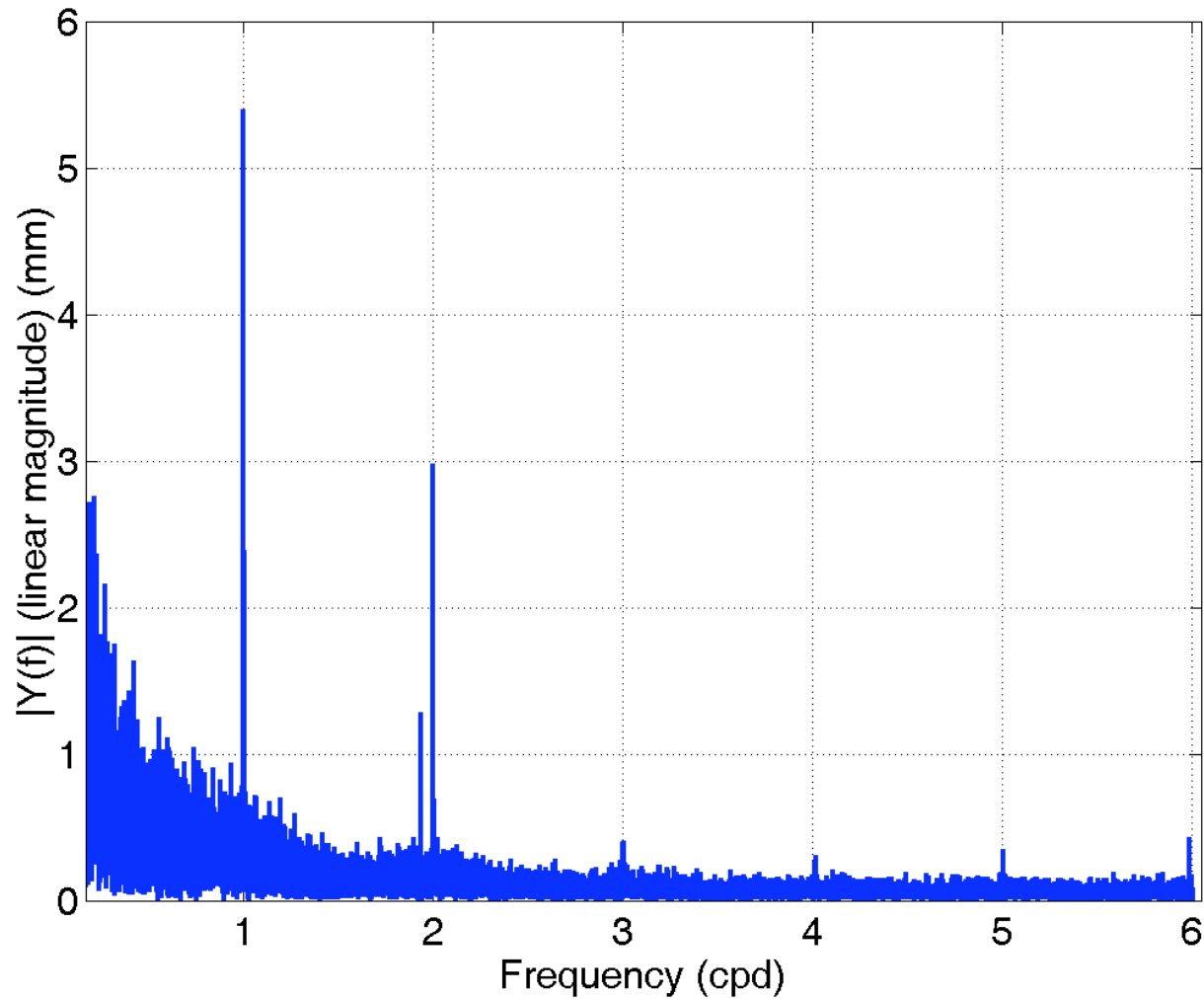
Power spectrum of BAHR time series



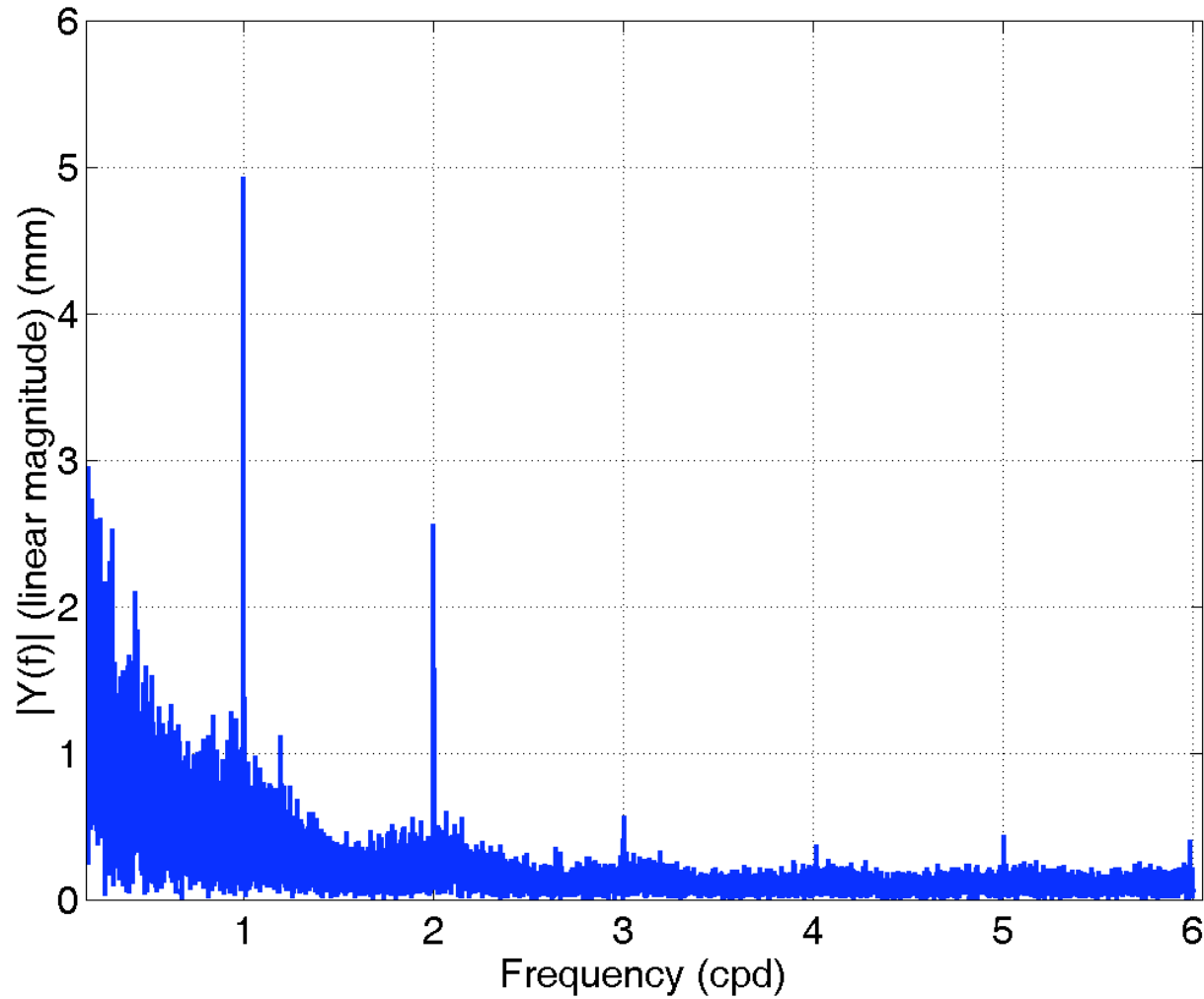
Comparison of ZND and surface pressure at BAHR



Cause for concern: L_2 at FORT 1997-2000



L_2 at FORT 2000-2004



Investigative approach

- Compare global distribution of ZND and surface pressure variations
- Focus on S2
 - Strong, zonally homogeneous pressure variation
 - Long wavelengths forgive sparse station coverage
 - S2 pressure variation is well characterized
- Use the new IGS ZND product
 - Higher sampling rate, lower formal errors compared to the legacy IGS ZND product
- Prefer reference frame sites

Analysis technique

- 1) Determine phase and amplitude of S2(ZND) at each site by a least-squares fit to the ZND time series

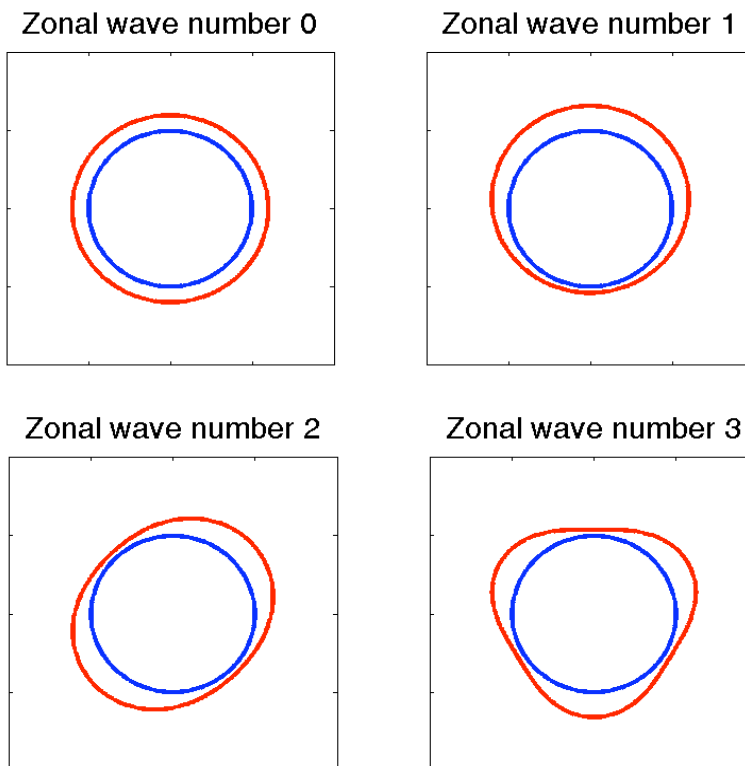
$$S_2(\tilde{\tau}^z) = A_2 \sin(2t' + \sigma_2) = a_2 \cos 2t' + b_2 \sin 2t'$$

- 2) Interpolate a_2 and b_2 to a regularly-spaced lat-long grid

- 3) Expand each line of latitude using a trigonometric series of longitude

This yields a decomposition of S2 into wave components:

$$S_2(t, \theta_i) = \sum_{-\infty}^{\infty} S_2^s(t, \theta_i)$$



Analysis technique

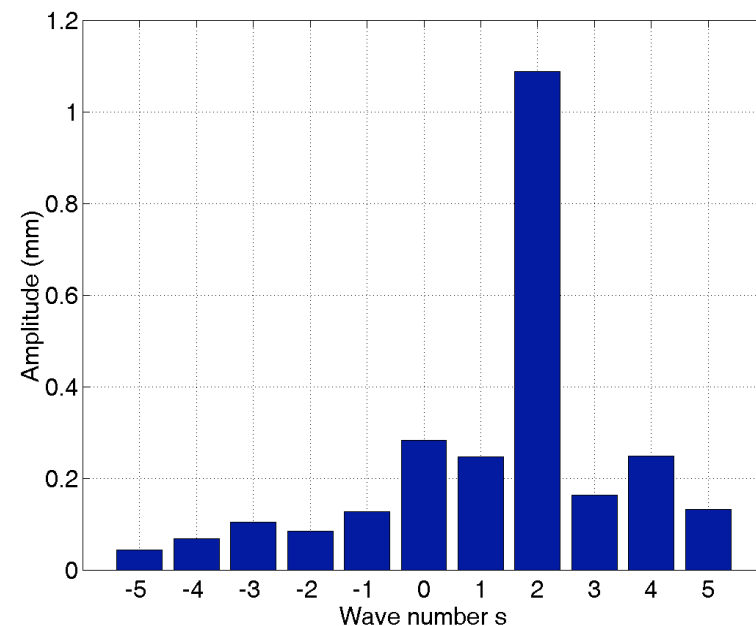
- 1) Determine phase and amplitude of S2(ZND) at each site by a least-squares fit to the ZND time series

$$S_2(\tilde{\tau}^z) = A_2 \sin(2t' + \sigma_2) = a_2 \cos 2t' + b_2 \sin 2t'$$

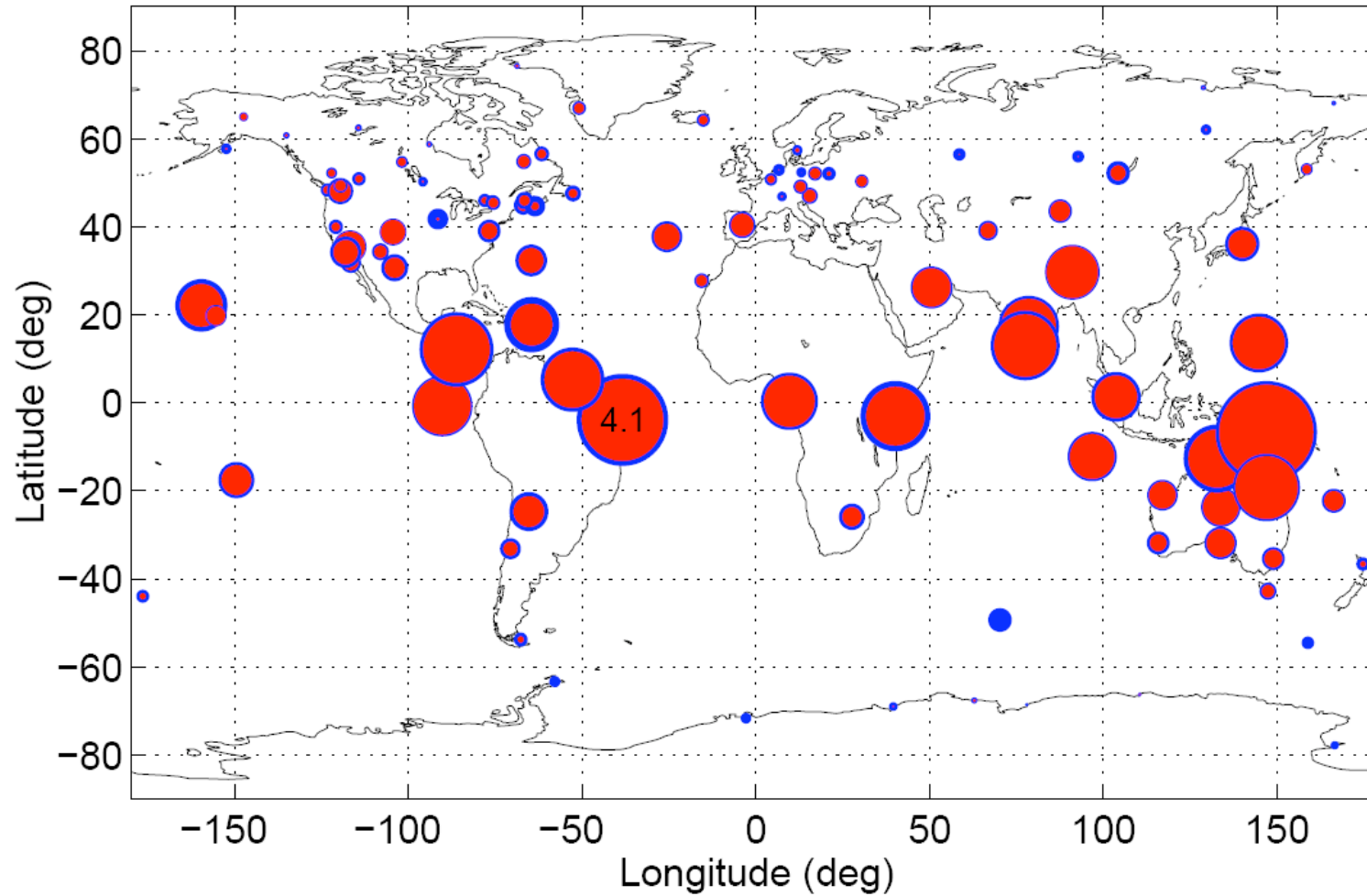
- 2) Interpolate a2 and b2 to a regularly-spaced lat-long grid
- 3) Expand each line of latitude using a trigonometric series of longitude

This yields a decomposition of S2 into wave components:

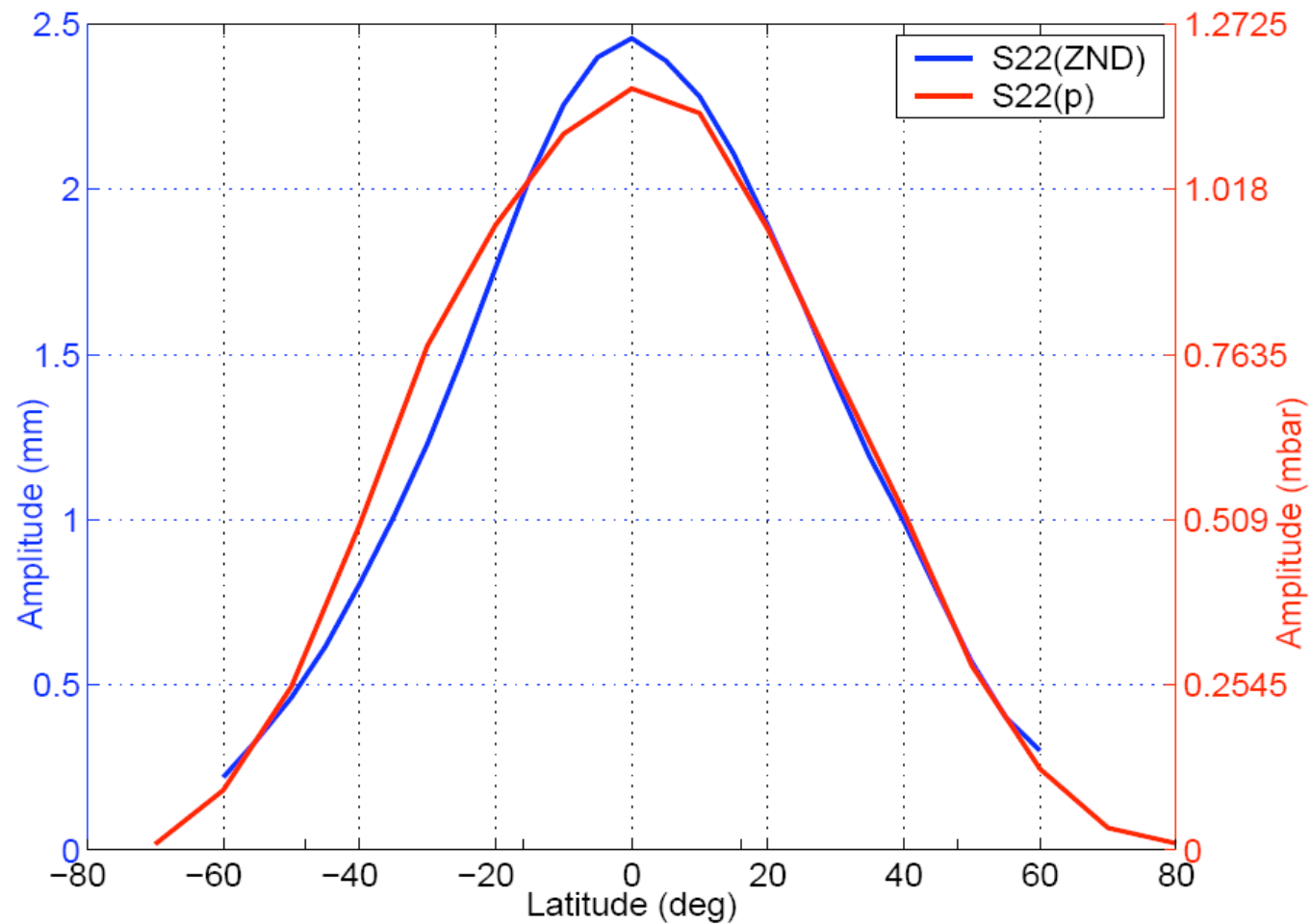
$$S_2(t, \theta_i) = \sum_{-\infty}^{\infty} S_2^s(t, \theta_i)$$



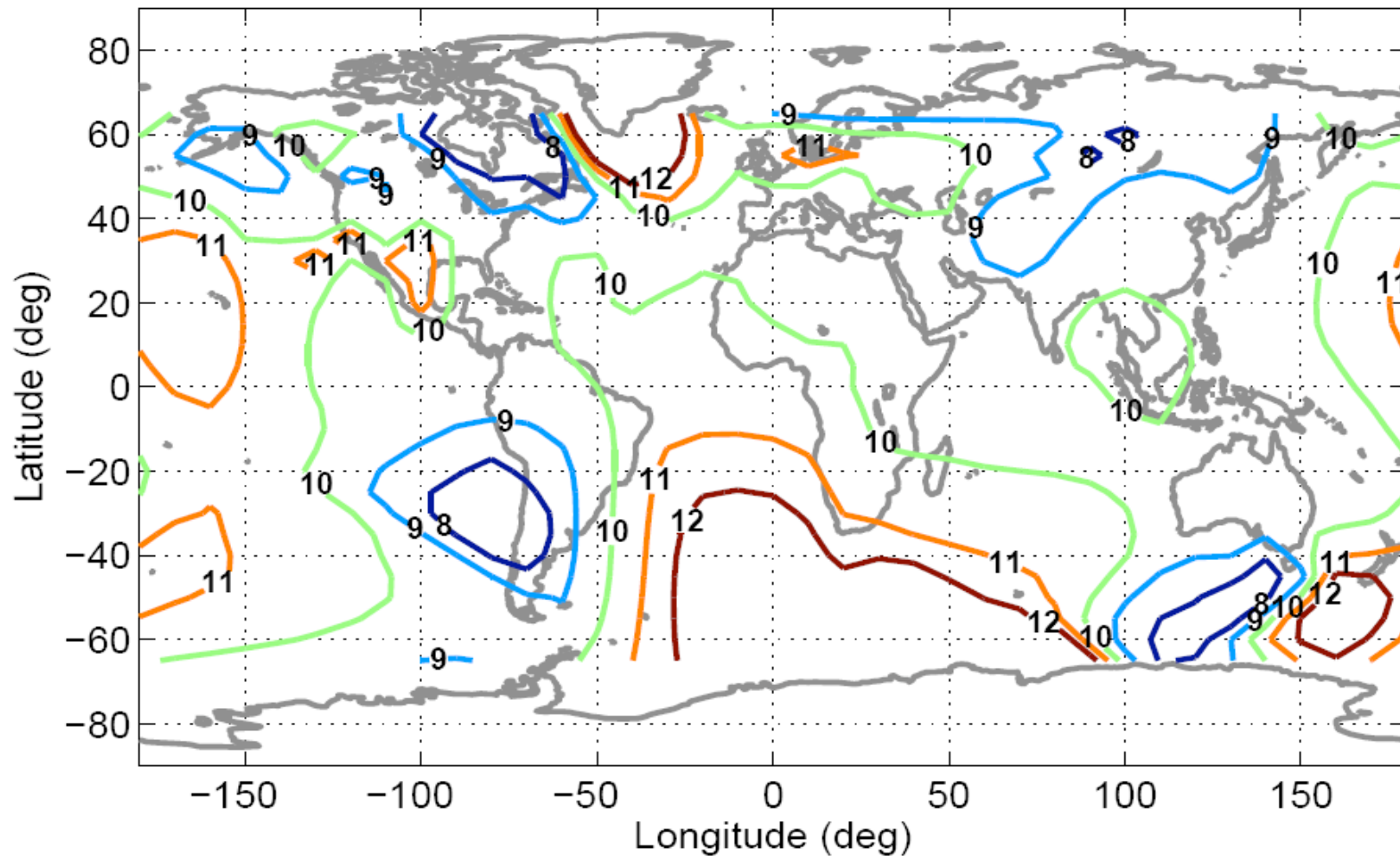
Results: S2(ZND) amplitudes



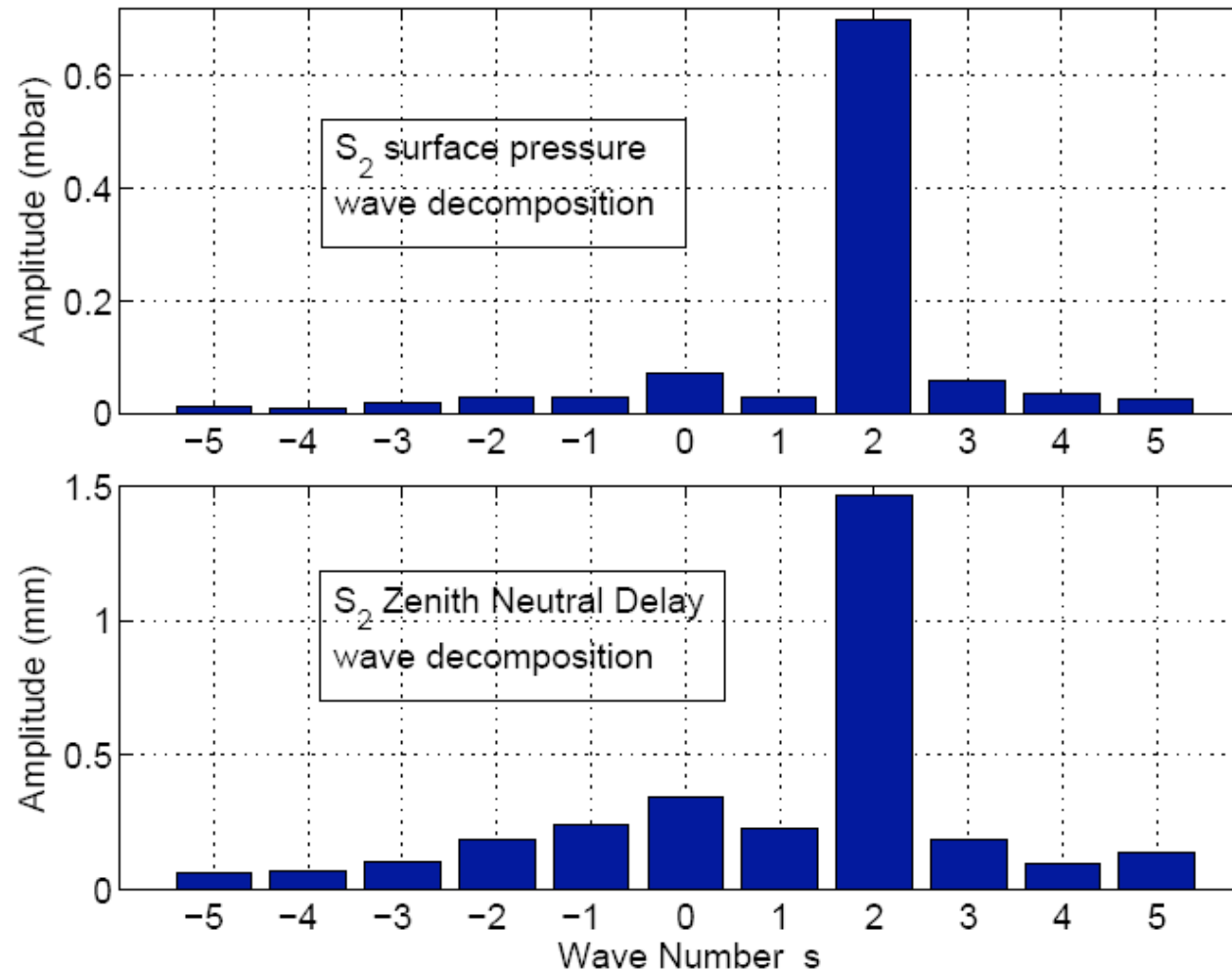
Latitudinal amplitude distribution: $S_{22}(ZND)$ vs. $S_{22}(p)$



S2(ZND) phase (expressed as LMST of first tidal maximum)



Wave decomposition: $S_2(\text{ZND})$ vs. $S_2(\text{p})$



Preliminary conclusions:

- S2(ZND) is strongly correlated with S2(p), suggesting that S2(ZND) is dominated by its hydrostatic component
- Unlikely that S2(ZND) is caused primarily by variations in EOP, ocean tide loading, solid earth tides, or IGS orbit/clock estimates

Further considerations:

- Precision of the S2(ZND) estimate
- Other possible error sources
 - Atmospheric loading
 - Mapping function errors

Precision of the S2(ZND) estimate

Site-by-site comparison: S2(ZND) vs. S2(p)

Station Data				ZND		MET	
Site	Lon	Lat	Ht	A_2	σ_2	A_2	σ_2
YELL	246	63	181	27 ± 5	157 ± 29	–	–
POTS	13	52	174	27 ± 6	148 ± 8	32 ± 1	142 ± 2
WTZR	13	49	666	60 ± 9	134 ± 16	36 ± 1	143 ± 1
ALGO	282	46	202	48 ± 14	200 ± 20	–	–
GOLD	243	35	987	149 ± 12	148 ± 3	–	–
JPLM	242	34	424	131 ± 14	84 ± 9	69 ± 1	150 ± 1
MDO1	256	31	2005	111 ± 18	91 ± 8	70 ± 1	154 ± 1
LHAS	91	30	3622	249 ± 19	156 ± 15	106 ± 2	157 ± 1
BAHR	51	26	–17	190 ± 12	162 ± 1	87 ± 1	160 ± 1
KOKB	200	22	1167	224 ± 6	92 ± 2	86 ± 1	164 ± 1
MKEA	205	20	3755	96 ± 10	118 ± 3	83 ± 1	161 ± 1
TOW2	147	–19	87	303 ± 18	154 ± 1	125 ± 2	163 ± 1
HRAO	28	–26	1414	107 ± 16	135 ± 7	–	–

^aLongitude in deg. E, latitude in deg. N, height in m, ZND amplitude in 10^{-2} mm, pressure amplitude in 10^{-2} mb, phase in deg. Error bounds are 1σ values.

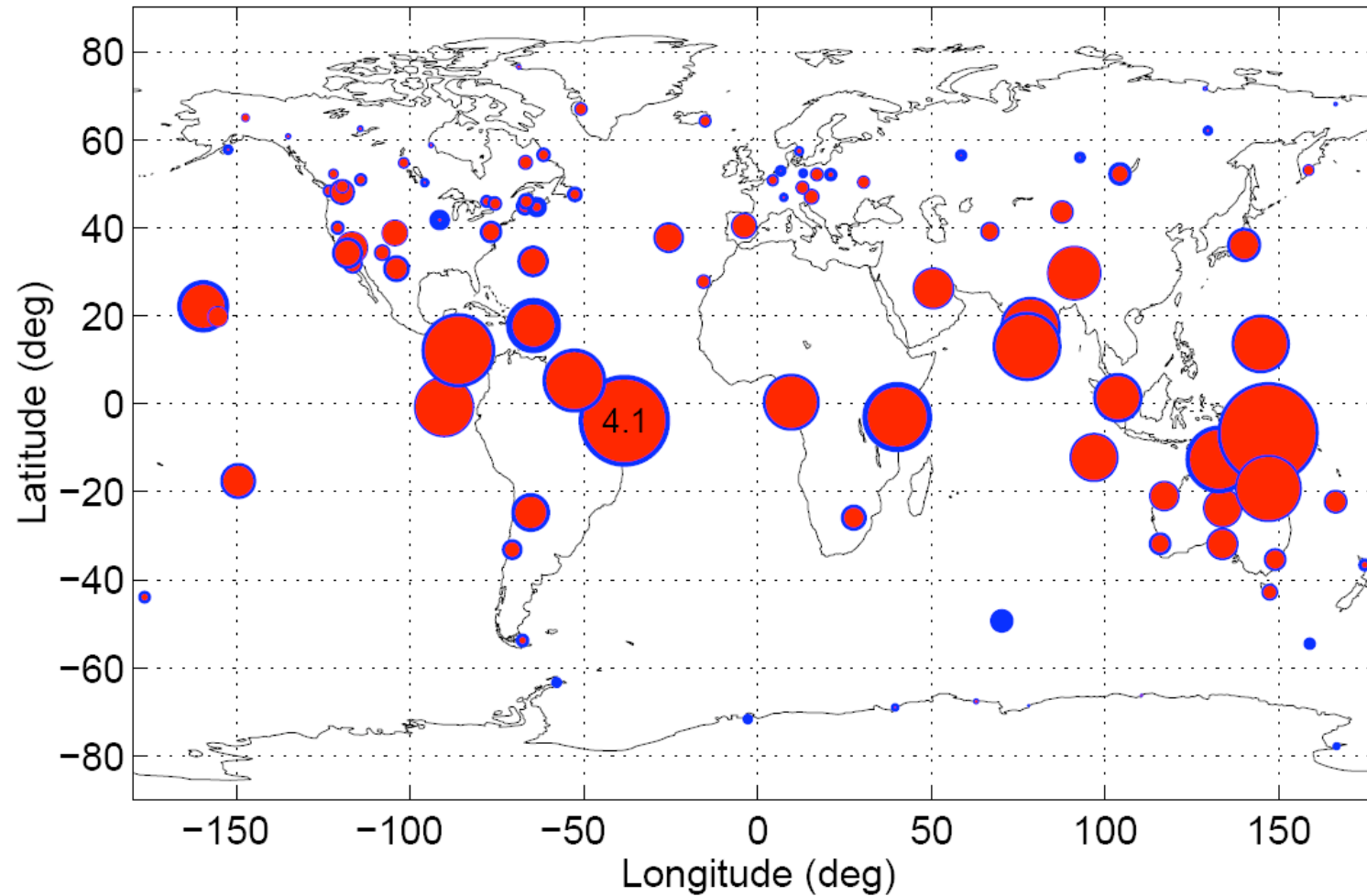
Precision of the $S2(\text{ZND})$ estimate

Site-by-site comparison: $S2(\text{ZND})$ vs. $S2(\text{p})$

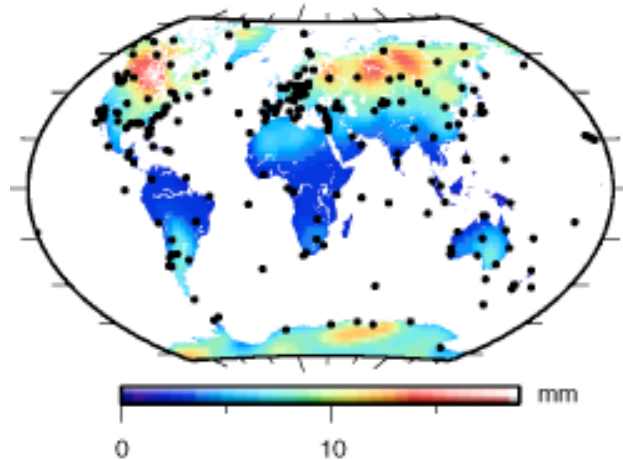
Station Data				ZND		MET	
Site	Lon	Lat	Ht	A_2	σ_2	A_2	σ_2
YELL	246	63	181	27 ± 5	157 ± 29	–	–
POTS	13	52	174	27 ± 6	148 ± 8	32 ± 1	142 ± 2
WTZR	13	49	666	60 ± 9	134 ± 16	36 ± 1	143 ± 1
ALGO	282	46	202	48 ± 14	200 ± 20	–	–
GOLD	243	35	987	149 ± 12	148 ± 3	–	–
JPLM	242	34	424	131 ± 14	84 ± 9	69 ± 1	150 ± 1
MDO1	256	31	2005	111 ± 18	91 ± 8	70 ± 1	154 ± 1
LHAS	91	30	3622	249 ± 19	156 ± 15	106 ± 2	157 ± 1
BAHR	51	26	–17	190 ± 12	162 ± 1	87 ± 1	160 ± 1
KOKB	200	22	1167	224 ± 6	92 ± 2	86 ± 1	164 ± 1
MKEA	205	20	3755	96 ± 10	118 ± 3	83 ± 1	161 ± 1
TOW2	147	–19	87	303 ± 18	154 ± 1	125 ± 2	163 ± 1
HRAO	28	–26	1414	107 ± 16	135 ± 7	–	–

^aLongitude in deg. E, latitude in deg. N, height in m, ZND amplitude in 10^{-2} mm, pressure amplitude in 10^{-2} mb, phase in deg. Error bounds are 1σ values.

$S2(ZND)$ amplitude distribution



Atmospheric pressure loading



Max pk-pk displacements in 2004
(Tregoning et al., GRL 2005)

ZND sensitivity to APL depends on several factors:

- 1) Spatial extent and amplitude of pressure anomaly
- 2) Distribution of ground sites
- 3) APL response at each site
- 4) ZND estimation strategy



CAS1

Constellation and ground station (CAGS) simulator/estimator

State vector:

$$X = \begin{bmatrix} R_1 \\ V_1 \\ R_2 \\ V_2 \\ \vdots \\ R_{n_{sv}} \\ V_{n_{sv}} \\ r_1 \\ r_2 \\ \vdots \\ r_{n_s} \\ \tau_1^z \\ \tau_2^z \\ \vdots \\ \tau_{n_s}^z \end{bmatrix}$$

State dynamics model:

$$X(k+1) = f[X(k), v(k)]$$

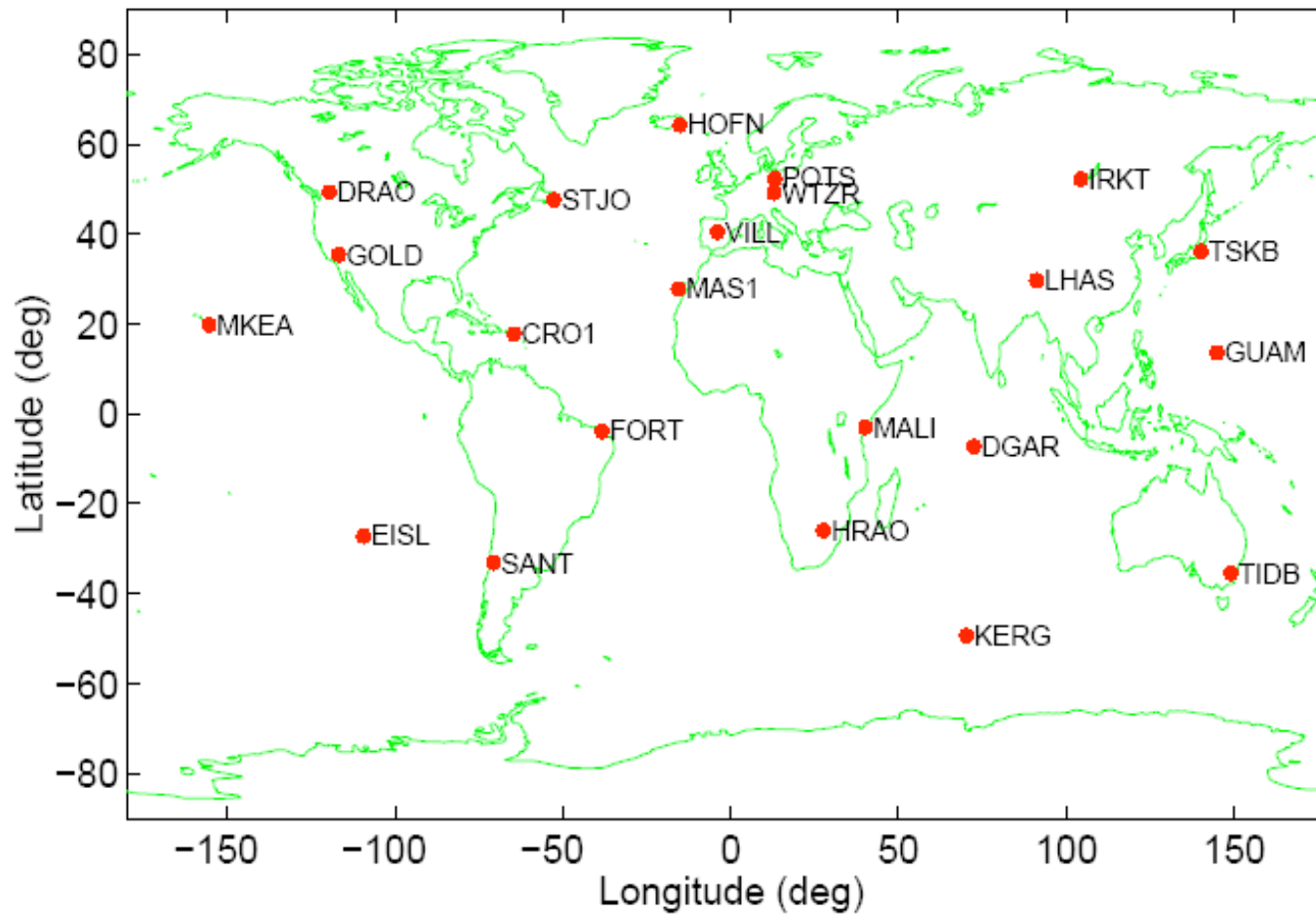
Nonlinear measurement model:

$$Z = \begin{bmatrix} \tilde{\rho}_1 \\ \tilde{\rho}_2 \\ \vdots \\ \tilde{\rho}_{n_z} \end{bmatrix} \quad \tilde{\rho}_i = \rho_i + \text{csc}(E_i)\tau_i^z$$

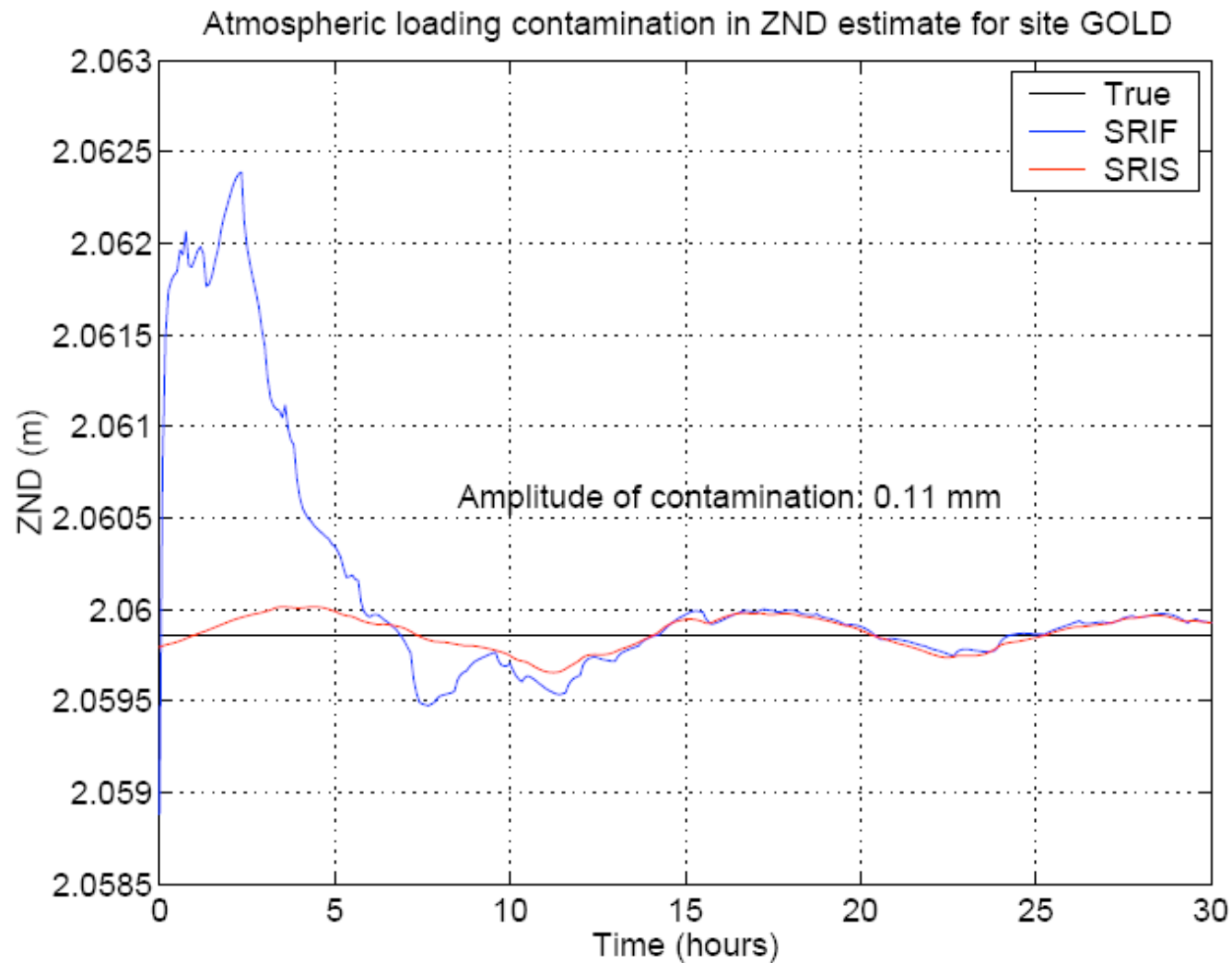
$$Z(k) = h[X(k)] + w_z(k)$$

Implementation: Square-root information filter/smoothen with a 30-h data arc

Sites used in the CAGS simulator/estimator



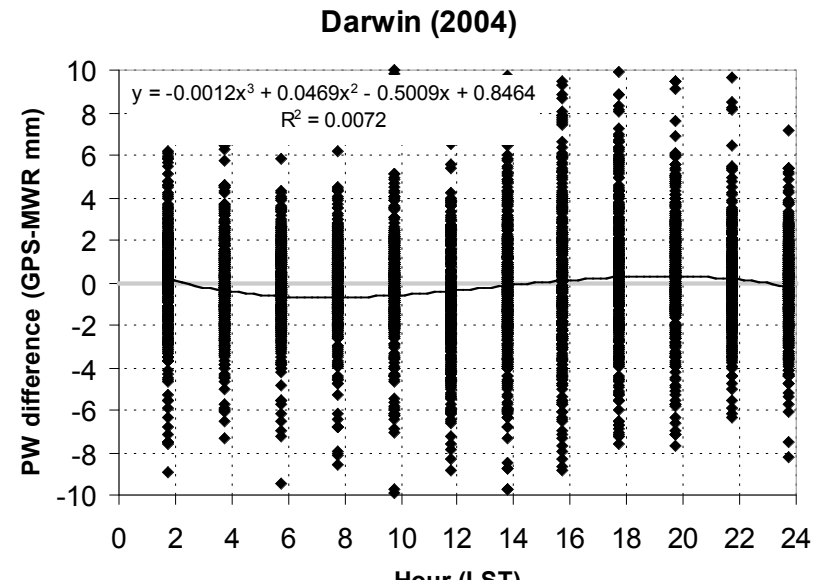
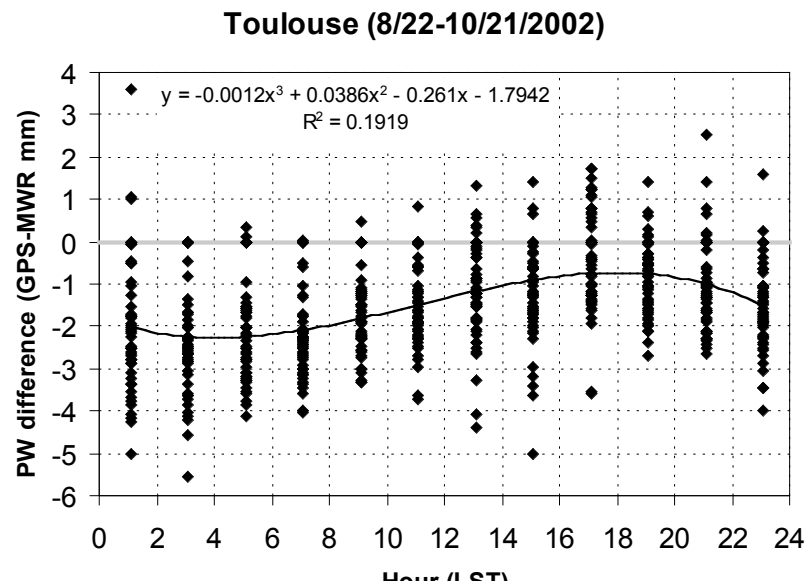
CAGS results



Mapping function errors

- IGS currently uses the Neill mapping function
 - Neill (1996) showed that radiosonde-derived “truth” mapping functions exhibit a diurnal variation at low elevation angles
 - Because the NMF does not account for variations on these short time scales, this leads to a 1% diurnal error in the hydrostatic NMF at 5 deg elevation
 - Amounts to a spurious 0.5 mm diurnal, <0.17 mm semidiurnal variation in GPS-derived ZND

GPS and MWR estimates of PWV provide evidence for diurnal mapping function errors



Figures provided by Junhong Wang
NCAR/EOL

Summary

- A strong global correlation between $S2(p)$ and $S2(ZND)$ as present in IGS data suggests that the latter is due primarily to the actual semidiurnal variation in ZND and not to modeling or other errors
- APL and Neill MF errors contribute less than 11% each to the apparent $S2(ZND)$
- Local incongruities may indicate the effects of water vapor or site-dependent errors, these invite further study

Acknowledgements

Thanks to Jim Ray for many useful discussions and to Paul Tregoning for careful comments in review.

Thanks to Junhong Wang and Aiguo Dai for useful discussions and figures.

Work supported in part by the Office of Naval Research and by the National Science Foundation.